Elemental Abundances in NGC 3516

T. J. Turner[1,2], S. B. Kraemer[3,4], R. F. Mushotzky[2], I. M. George[1,2], J.R. Gabel[3,4]

ABSTRACT

We present Reflection Grating Spectrometer data from an *XMM-Newton* observation of the Seyfert 1 galaxy NGC 3516, taken while the continuum source was in an extremely low flux state. This observation offers a rare opportunity for a detailed study of emission from a Seyfert 1 galaxy as these are usually dominated by high nuclear continuum levels and heavy absorption. The spectrum shows numerous narrow emission lines (FWHM $\lesssim$ 1300 km s^{-1}) in the 0.3 – 2 keV range, including the H-like lines of C, N, and O and the He-like lines of N, O and Ne. The emission-line ratios and the narrow width of the radiative recombination continuum of Cvi indicate that the gas is photoionized and of fairly low temperature ($kT \lesssim 0.01$ keV). The availability of emission lines from different elements for two iso-electronic sequences allows us to constrain the element abundances. These data show that the N lines are far stronger than would be expected from gas of solar abundances. Based on our photoionization models we find that nitrogen is overabundant in the central regions of the galaxy, compared to carbon, oxygen and neon by at least a factor of 2.5. We suggest that this is the result of secondary production of nitrogen in intermediate mass stars, and indicative of the history of star formation in NGC 3516.

Subject headings: galaxies: active – galaxies: individual (NGC 3516) – galaxies: nuclei – galaxies: Seyfert – galaxies: abundances

1. Introduction

X-ray and UV spectra of the Seyfert 1 galaxy NGC 3516 (z=0.008836±0.000023, Keel 1996) have shown evidence for a significant column of ionized gas along the line-of-sight to

---

[1]Joint Center for Astrophysics, Physics Dept., University of Maryland Baltimore County, 1000 Hilltop Circle, Baltimore, MD 21250

[2]Laboratory for High Energy Astrophysics, Code 662, NASA/GSFC, Greenbelt, MD 20771

[3]Catholic University of America, NASA/GSFC, Code 681, Greenbelt, MD 20771

[4]Laboratory for Astronomy and Solar Physics, Code 681, NASA/GSFC, Greenbelt, MD 20771

the nucleus (Kriss et al. 1996; Netzer et al. 2002; Kraemer et al. 2002). A recent *Chandra* observation of this source found it to exist at a historical low-state. The spectrum at that epoch, and comparison with previous X-ray data led Netzer et al. (2002) to suggest a model for NGC 3516 where a constant column of gas reacts to changes in the nuclear ionizing flux. That gas was constrained to have density $> 2.4 \times 10^6 cm^{-3}$ and exist at a distance $< 6 \times 10^{17} h_{75}^{-2}$ cm from the nucleus. Netzer et al. (2002) also detected a strong Ovii 0.561 keV line and marginally detected a Nvi 0.419 keV line. Line measurements from the *Chandra* Low Energy Transmission Grating (LETG) data appeared consistent with emission from the X-ray absorber.

We present here *XMM-Newton* (hereafter *XMM*) RGS grating spectra of NGC 3516. These data allow us to rethink the origin of the X-ray line emission in NGC 3516.

2. The *XMM* RGS Observation

An *XMM* observation of the Seyfert 1 galaxy NGC 3516 was performed covering November 09 UT 23:12:51 – 11 UT 10:54:19. This observation was part of a multi-satellite campaign which including overlapping observations by *RXTE* and *Chandra*. The Fe Kα line shows interesting structure and evolution during the observation, and the combined data in the hard X-ray regime are detailed by Turner et al. (2002). Here we present a detailed analysis of the *XMM* RGS grating data from 2001 November.

As noted by Turner et al. (2002) NGC 3516 had a flux $F_{2-10\ keV} \sim 1.3 - 1.5 \times 10^{-11} erg\ cm^{-2}\ s^{-1}$, during the November 2001 observations. The source was in this flux state during the previous *Chandra* LETG observation (Netzer et al. 2002) and as observed by *ASCA* during 1999 (Figure 1). Unfortunately no useful RGS data were obtained from an earlier epoch observation with *XMM* in 2001 April, due to background flares during a period of high solar activity.

RGS data were processed using the SAS 5.3.3. version of RGSPROC and spectra were extracted using standard regions (the source cell encompassing 97% of the cross-dispersed counts) and extraction criteria, resulting in exposure times $\sim$ 114 ks in RGS-1 (R1) and $\sim$ 108 ks in RGS-2 (R2). The full-band (0.34-2.0 keV) RGS background-subtracted count rates were 0.062 ± 0.0008 (R1) and 0.067 ± 0.0008 (R2). The background comprised 17% of the total count rate in R1 and R2, respectively. We note that due to problems with some of the CCD chips onto which the RGS spectrum is dispersed there are two prominent data gaps evident, R1 has a gap between $\sim$ 0.9-1.2 keV and R2 has a gap between $\sim$ 0.51 - 0.62 keV. We note that in this analysis we adopted cz=2649 km/s Keel (1996).

Ignoring emission and absorption lines for the moment, we find a good parameterization of the continuum shape in RGS data over the 0.3 - 2 keV band using a powerlaw of photon index $\Gamma = 2.17^{+0.04}_{-0.06}$ attenuated by a Galactic column of cold gas $N_H = 2.9 \times 10^{20} \mathrm{cm}^{-2}$ plus a column of ionized gas with $N_{H(UV)} = 7.7 \times 10^{21} \mathrm{cm}^{-2}$. Such a column of ionized gas is expected from the UV and LETG analyses (Netzer et al. 2002; Kraemer et al. 2002) of data from an epoch close in time to these RGS data (and the ionized gas is modeled using CLOUDY90 for solar abundance material, Ferland et al. 1998). Inclusion of the ionized gas improves the fit from $\chi^2 = 1594/639$ *dof* to $1180/638$ *dof* and provides a good model to the gross shape of the soft spectrum. Figure 2 shows the data compared to this model. However, our parameterization of the continuum shape is not the only possible model. A recent alternative applied to some Seyfert spectra parameterizes broad spectral wiggles as emission lines due to ionized material in the accretion disk (e.g. Branduardi-Raymont et al. 2001). However, we do not pursue such a parameterization in this paper. The absorption edges expected from the (previously observed) ionized absorber provide a good description of most of the broad features, and we believe this makes our interpretation of the spectrum a compelling way to proceed for this observation of NGC 3516.

The most immediate result evident from Figure 2 is that the RGS spectra show several prominent emission lines. The two strongest lines are those at 0.4198 keV and 0.5614 keV. We identify these with forbidden components of Nvi and Ovii, respectively. These two strong lines were measured carefully to determine bulk and turbulent velocities of the emitting gas. For the Nvi line we measured a rest-energy $E = 419.8 \pm 0.2$ eV and for the Ovii line $E = 561.4 \pm 0.3$ eV. Errors are 90% confidence. Intrinsic line widths were found to be $\sigma = 3.8^{+3.5}_{-3.8} \times 10^{-4}$ keV and $\sigma = 5.6^{+4.4}_{-5.6} \times 10^{-4}$ keV, respectively. The energy for Ovii f corresponds to blueshift of 214^{+160}_{-80} km/s while for Nvi the blueshift is 143^{+143}_{-143} km/s, i.e. consistent with no blueshift. For comparison, the absolute wavelength calibration for the RGS is ~ 8m Å, or ~ 100 km/s at 0.5610 keV. Thus the evidence for a blueshift for the Ovii line is marginal, the lower limit is close to the accuracy of the detector absolute wavelength calibration. The line widths correspond to velocities FWHM(Nvi) $= 646^{+581}_{-646}$ km/s and FWHM(Ovii) $= 704^{+554}_{-704}$ km/s. Line widths are consistent with zero, the upper limits constrain velocity broadening to $\lesssim 1300$ km/s. (For comparison the FWHM resolution of R1 is ~ 680 km/s at the observed energy of Nvi, 0.416 keV and ~ 850 km/s at the observed energy of Ovii, 0.556 keV). Changes in the detector effective area with energy cause some apparent asymmetries at first glance as the effective area changes significantly across some line profiles (e.g. Oviii at 0.654 keV). However we find no true asymmetry in any emission line profile.

To search for weak emission lines we slid a Gaussian template across the data, testing for an improvement to the fit at every resolution element compared to our model of the

underlying continuum. The data were first binned by a factor of 8 to a binsize of 0.32 Å to ensure that there were greater than 20 photons in each spectral bin so χ^2 fitting could be employed. Examination of the RGS background spectra shows a broad bump centered around 0.39 keV (not fully understood but thought likely due to relatively high dark current in CCD2 for both RGS instruments; XMM Users Handbook, also see den Herder et al. 2001). Other known features in the RGS background include emission from Al Kα close to 1.5 keV, due to Al in the detector housing. This means we need to subtract the RGS background to ensure we isolate the spectral properties of the source. Figure 3 shows the results of this sliding Gaussian test against the observed data in red. Plotted is the improvement in the fit-statistic. This the plot is useful in assessing the *significance* of each line, but not the strength of the line. It can be seen that the addition of an emission feature results in a large improvement in χ^2-statistic at several energies.

In order to assess the reality of these features, we have constructed a series of simulated datasets. For each RGS, 20 separate background spectra were generated by randomly adding the appropriate Poisson noise to each channel in the observed background spectrum. Similarly, 20 simulated source spectra were generated for each RGS, again with Poisson noise introduced, using our model of the underlying continuum convolved with the instrumental response. These simulated data sets were then combined and 20 R1+R2 pairs analysed in the same manner as the observed spectra above. Specifically, the sliding Gaussian test was performed for each of the 20 pairs, and the maximum reduction in fit-statistic at each energy noted. The result is plotted in blue in Figure 3, and therefore represents a 95% significance threshold at each energy (and takes into account all instrumental and background features).

Including the Nvi and Ovii lines discussed above, we find a total of 13 emission features (some of which are blends) in the observed spectrum above the 95% confidence threshold. Ten of these 13 occur at energies consistent with atomic transitions of abundant ions, and have understandable intensity ratios (below). Thus we consider these 10 feature to be robust detections. They are labeled on Figure 3 and listed in Table 1. Of the remaining three features, that at 0.39 keV is most likely due to the detector background described above. The final two features (at 0.697 and 0.706 keV; and apparent strengths corresponding to $\sim 0.4 \times 10^{-5}$ photons cm^{-2} s^{-1}) do occur at energies close to atomic transitions. The former, is consistent with the Ovii ($1s^2 \rightarrow 1s4p$) resonance line at 0.698 keV. However, the lack of any indication of the Ovii ($1s^2 \rightarrow 1s3p$) line at 0.665 keV makes such an interpretation extremely unlikely. The line at 0.706 keV could be identified with Sxiv RRC at 0.707 keV. However, such an interpretation would lead us to expect a much stronger Oviii RRC at 0.871 keV than observed. In summary, only the 10 emission lines which we believe secure ($\delta\chi^2 > 10$) and attributable to NGC 3516 appear in Table 1.

While some of the detected features have some significant width, e.g. the CvI RRC, the features were too weak for us to fit for the width and thus the temperature of the emitting gas. However we did obtain an upper limit on width, $kT \lesssim 0.01$keV, i.e. $T \lesssim 120,000$K. This is consistent with the width of the RRC features in NGC 1068, based on which Kinkhabwala et al. (2002) argued that the X-ray emitting plasma was purely photoionized.

The emission lines were assumed to originate outside of the UV absorber (i.e. not absorbed by it). If the emitter were inside the UV absorber it would have to reside within 10^{16} cm of the nucleus with a density 10^9 cm^{-3} or so (Kraemer et al. 2002). While such a location is possible, the velocity widths of the emission lines at FWHM< 1300 km/s are rather narrow for such a small radial location. These widths are more suggestive of an origin on the pc-scale. Furthermore, some results from Seyfert 2 galaxies suggest the X-ray emitting gas in general has extent on the 10-100pc size-scale (e.g. Sako et al. 2000). All things considered, it seems most likely the emitting gas lies outside of the UV absorber in this case. The fact the absorption edges are imprinted on the soft spectrum must then be explained as the soft-band having a significant contribution from nuclear continuum emission, transmitted through the UV absorber (the fraction of the nuclear continuum scattered by the line-emitting gas is negligible, as shown in Section 3.2). Thus we suggest a full model of absorbed continuum component plus unabsorbed lines (with Galactic column absorbing all). The line fluxes in Table 1 are the inferred intrinsic fluxes at the source (i.e. corrected for Galactic absorption). In addition to tabulating the fitted line fluxes, we noted the total counts in the bin, those attributable to the continuum emission and thus those attributable to the emission line itself. Errors are calculated on the counts in the line and the same fractional errors are applicable to the fluxes listed.

The process was repeated to search for weak absorption lines. Following a similar process to that used to detect the emission lines, we found evidence for an absorption feature at 0.358 keV and broad features centered on 0.753 keV and 0.96 keV. The former has no obvious identification. The feature at 0.75 keV, while close to a jump in detector efficiency, appears real, and we identify this with the unresolved transition array due to inner-shell absorption by FeIX - XI M-shell ions, as observed in some other AGN (e.g. IRAS 13349+2438, Sako et al. 2001). The feature at $\sim$ 0.96 keV may be a blend of Fe lines from highly-ionized gas (Fe XX - XXIV). Much weaker features at 0.54 keV and 0.61 keV do not have clear identifications.

Absorption lines and edges were expected to be detected in NGC 3516 from transmission of the nuclear continuum through ionized gas, previously observed in this source (e.g., Kriss et al. 1996; Netzer et al. 2002; Kraemer et al. 2002). The overall shape of the RGS spectra shows the imprint of the absorption edges expected from the X-ray absorption associated with the gas measured by STIS (Kraemer et al. 2002). The width of the UV absorption lines

is $\sim 20 - 70$ km/s, X-ray absorption lines with the same velocity structure would be too narrow to detect with the RGS (or *Chandra* grating data).

3. FUSE data

We reduced data from an archival *Far Ultraviolet Spectroscopic Explorer (FUSE)* spectrum, originally obtained on 2000 April 17, again, while NGC 3516 was in an extremely low flux state (see Kraemer et al. 2002). From the *FUSE* spectrum we measured an Ovi λ 1038 flux of $\approx 1.6 \times 10^{-14}$ ergs s^{-1} cm^{-2}, with a FWHM of ~ 250 km s^{-1}. Given the intrinsic 2:1 emission ratio of Ovi λ 1032/ Ovi λ 1038, line fluxes the total Ovi flux should be $\sim 4.0 \times 10^{-14}$ ergs s^{-1} cm^{-2}. However, as noted by Hutchings et al. (2001) in their analysis of this spectrum, the observed Ovi doublet ratio is ~ 1:1, which they attributed to line transfer effects in optically thin gas. We think that it is more likely that the lines are absorbed by intervening gas, which may explain the asymmetric line profiles (see Hutchings et al. 2001) and the narrowness of the Ovi lines compared to the X-ray lines. However, it is not necessary that this absorption arises in the same material that produces the deep, variable X-ray absorption discussed in Netzer et al. (2002) and Kraemer et al. (2002), but could be a relatively small column of ionized gas (e.g., $\sim 10^{20}$ cm^{-2}, $U \sim 0.5$) that covers the NLR of NGC 3516. This component may only be detectable when viewed against the NLR emission, much of which was missed in the small $0''.2 \times 0''.2$ STIS aperture, but is well-covered by the $20''.0 \times 20''.0$ *FUSE* aperture. (At a distance of 35.7 Mpc for NGC 3516, $1'' = 173$pc.) In fact, similar evidence for absorbed UV narrow-line profiles has been seen in STIS spectra of NGC 1068 (Kraemer & Crenshaw 2000).

4. Physical Conditions in the Emission-Line Gas

4.1. Emission-Line Diagnostics

The dominance of X-ray emission lines in the soft spectrum of this Seyfert 1 galaxy is consistent with the low flux state of the source. If these lines have a $\sim$constant flux over years, then they would have been swamped by the nuclear emission at higher flux states.

This source is one of the few observed to date with detectable forbidden emission lines from 3 abundant elements in the He-like isoelectronic sequence (Nvi, Ovii and Neix). It is the first such case for a Seyfert 1 galaxy. Even at first glance, the emission line ratios look unusual. Compare for example the *XMM* RGS spectrum of NGC 3783 where the Nvi line was very weak compared to Ovii, as expected for solar abundance gas (Blustin et al. 2002).

The details of these anomalous line ratios are discussed, in the context of the photoionization models, in the following section.

As suggested by various authors (Pradhan et al. 1985; Liedahl 1999; Mewe 1999; Porquet & Dubau 2000), the physical conditions of photoionized plasmas can be constrained via the relative strengths of the most intense lines from He-like species; the resonance line ($1s^2\ ^1S_0 - 1s2p\ ^1P_1$), the two intercombination lines ($1s^2\ ^1S_0 - 1s2p\ ^3P_{2,1}$), and the forbidden line ($1s^2\ ^1S_0 - 1s2s\ ^3S_1$). The ratios of the forbidden line to the two intercombination lines (the R ratio) is sensitive to density, while the ratio of the sum of the forbidden and intercombination lines to the resonance line (the G ratio) is sensitive to electron temperature. If the resonance lines are relatively strong, the latter ratio can indicate temperatures in excess of those expected for a photoionized plasma. However, the resonance lines can be also be photo-excited (Sako et al. 2000), hence the G-ratio may not be a reliable indicator of either the temperature or means of excitation of the plasma. Based on their analysis of an *XMM-Newton* RGS spectrum of NGC 1068, Kinkhabwala et al. (2002) suggested that the excess emission in virtually all the detected resonance lines was the result of photo-excitation in a purely photoionized plasma.

In these data, the R ratio of the OVII f-line to the i-lines is ~ 3.5 (see Table 1), which for a photoionized plasma implies an electron density $n_e \sim$ several x 10^9 cm^{-3} (Porquet & Dubau 2000). However, the weakness of the intercombination lines, plus any underlying contribution from the wings of the adjacent forbidden and resonance lines, can easily lead to an overestimate of the flux. Hence, it is likely that n_e is lower. Furthermore, at sufficiently high density, the metastable $1s2s\ ^3S_1$ level begins to collisionally depopulate, suppressing the forbidden line of the He-like triplet. For NVI this occurs at $n_e > 10^8$ cm^{-3}, while the depopulation of corresponding OVII level occurs at densities $\sim$ factor of 10 greater (Porquet & Dubau 2000). Given the relative strengths of the NVI and OVII forbidden lines, we suggest that the average density in the emission-line gas is $n_e \lesssim 10^8$ cm^{-3}.

4.2. Photoionization Models

Photoionization models of the X-ray emission-line gas were generated using the Beta 5 version of CLOUDY (Gary Ferland, private communication). This version of the code includes new atomic data for the He-like ions. We modeled the emission-line gas as a single-zoned slab of atomic gas, irradiated by the central source, for which we used the same spectral energy distribution and luminosity ($\sim 10^{43}$ erg s^{-1}) described in Kraemer et al. (2002). As usual, the models are parameterized in terms of the ionization parameter U, which is the ratio of ionizing photons per H atom at the ionized face of the slab. We *initially* assumed

solar elemental abundances (Grevesse & Anders 1989), which are, by number relative to H, as follows: He = 0.1, C = 3.4 x 10^{-4}, N = 1.2 x 10^{-4}, O = 6.8 x 10^{-4}, Ne = 1.1 x 10^{-4}, Mg = 3.3 x 10^{-5}, Si = 3.1 x 10^{-5}, S = 1.5 x 10^{-5}, and Fe = 4.0 x 10^{-5}. The gas was assumed to be free of dust.

Prior to generating new models, we explored the possibility that the X-ray emission lines arise in the UV/X-ray absorber described in Kraemer et al. (2002). In the current low-flux state of NGC 3516, the models of the strongest UV components predicted ratios of ionic columns for Ovi:Ovii:Oviii to be roughly 1.00:0.67:0.03. Consequently, little Oviii Lyα emission is expected relative to Ovii emission for the UV gas seen in emission. This is not the case, we observe enough Oviii emission to know there must be an additional component of higher-ionization gas present. We also note the model for the production of Ovi $\lambda\lambda$ 1032,1038 emission lines from the UV gas yields fluxes $\sim$ 20 times as strong as the Ovii f-line. In the data they appear weaker than this, as noted further below.

Since the X-ray emission-lines cannot be formed in the UV/X-ray absorbers, we permitted U and the total column density (N_H = Hi + Hii) to vary, as a new model is required for the X-ray emitting gas. In Table 2, we compare the model predictions to the measured emission-line fluxes by scaling the predicted Ovii f-line flux to that observed. We find that line ratios can be roughly matched using a single-zoned model, with U = 1.1, N_H = 1.5 x 10^{21} cm^{-2}, and solar abundances (Model 1). In order to boost the strength of the resonance lines via photo-excitation, we introduced a turbulent velocity of 50 km s^{-1}, which is roughly equal to the average FHWM of the individual UV absorbers (Kraemer et al. 2002). If we assume n_e = 10^8 cm^{-3}, our model results place the emission-line gas at a radial distance of 0.02 pc; although this is within the range determined for the UV absorbers, since the lower limit to the density is not well constrained. It is quite plausible that the emission-line gas lies further from the nucleus, as we discussed in Section 2. The model predicts a mean electron temperature of 7.4 x10^4K, in agreement with the constraints determined from the Cvi RRC.

The model predictions assuming solar abundance are within the measurement errors for the Ovii He-like lines, Neix f, and Oviii Lyα, while the prediction for Cvi Lyα is slightly high. However, the strengths of the Nvi He-like lines and Nvii Lyα line are unpredicted by factors of $\sim$ 4 and $\sim$ 2, respectively, which is strong evidence against our initial assumption of solar abundances. The apparently anomalous line ratios in NGC 3516 suggests one of two possibilities; the other elements such as C and O are depleted onto dust grains (e.g. Shields & Kennicutt 1995), or the N abundance exceeds the Solar value.

Considering the case of depletion onto dust grains. UV data show many cases of enhanced nitrogen relative to carbon, e.g. NGC 5548 (Crenshaw et al. 2003) and Akn 564 (Crenshaw et al. 2001). In those cases C may be depleted onto dust grains. However, in

NGC 3516 the data argue against dust depletion. While the ratio of N/C is high, the ratio N/O is also high and yet O is not heavily depleted onto dust grains (see Snow & Witt 1996). Also the ratio N/Ne is high and Ne cannot be depleted onto dust grains. Thus we rule out depletion.

Hence, it is most likely that nitrogen is over-abundant, perhaps by a factor of 2 – 3. Interestingly, Kinkhabwala et al. 2002 came to a similar conclusion for NGC 1068. As a result, we regenerated the model using a N/H ratio of 2.5 x solar (Model 2). As shown in Table 2, the fit for the Nvii line is quite good. While the Nvi lines are much closer to the observed strengths, they are still somewhat underpredicted. The latter may simply be a reflection of the difficulty in matching the emission lines with a single-zone model, since some additional Nvi could arise in a component of lower ionization gas. Our discovery of nitrogen overabundance led us to revisit the absorber used which fits the UV data and models the broad features in the soft X-ray band. First we note that the STIS data on which that absorber was based (Kraemer et al. 2002) showed saturated N and C lines, so limits from those lines did not provide tight constraints on the state of the gas for the UV model. Fine-tuning abundances for the absorber model does not make any significant difference to the fit to broad features and thus to the emission line analysis and conclusions drawn here.

Based on the model predictions, we can constrain the global covering factor of the emission-line gas. Our predicted flux for Ovii f emitted from the illuminated face of the photoionized slab is 1.7 x 10^5 ergs cm^{-2} s^{-1}. Adopting a distance of 35.7 Mpc for NGC 3516, assuming H_o = 75 km s^{-1} Mpc^{-1} (Ferruit, Wilson & Mulchaey 1998), the total O VII f emission from NGC 3516 is $\approx$ 5.5 x 10^{39} ergs s^{-1}. Hence, the emitting surface area must be $\approx$ 3.2 x 10^{34} cm^2. Based on our assumed density, n_e=10^8 cm^{-3}, and luminosity in ionizing photons, the emission-line gas lies at a radial distance of 6.9 x 10^{16} cm, which yields a total surface area of 6.0 x 10^{34} cm^2. Hence the covering factor of the emission line gas is $F_c \sim$ 0.5. While we expect that the emission-line gas extends over a range in radial distance, and hence density, the total covering factor will be similar.

From the predicted covering factor and column density, we can determine the fraction of the nuclear continuum reflected via electron scattering within the emission-line gas. Assuming isotropic scattering, at small electron-scattering optical depths $\tau_e < 1$, the reflected fraction of continuum radiation $f_r \approx N_{electron} F_c \sigma_T$, where $N_{electron}$ is the electron column density ($\approx N_H$) and σ_T is the Thomson cross-section. We find $f_r \approx$ 5 x 10^{-4}, hence a negligible fraction of continuum radiation will be scattered into our line-of-sight by this component.

Returning to the question of the strength of Ovi emission. The total Ovi flux derived from the *FUSE* data is $\sim$ 4.0 x 10^{-14} ergs s^{-1} cm^{-2}. Our X-ray emission-line model predicts

a total Ovi flux of 6.75 x 10^{-14} ergs s^{-1} cm^{-2}, which, since it is somewhat higher than the *FUSE* value, may support the indication (from the doublet ratio) that these lines are absorbed. Under the assumption that the strengths of the emission lines are constant this Ovi measurement provides a tight constraint on the ionization state of the NLR gas in which the UV and optical emission-lines arise.

5. Discussion

The relation between abundance and AGN redshift, luminosity, and the inter-relation between the AGN and starburst regions are key to understanding AGN formation and evolution. Based on the ratios of the Nv λ 1240 emission line to Civ λ 1550 and HeII λ1640, it has been argued that QSOs show high metallicity (Z$\geq$ 1, where Z = 1 for solar abundances) and, in particular, high N abundance at redshifts as high as $z \geq 3$, indicative of enrichment due to rapid star formation at epochs as early as $\leq$ 1 Gyr (Hamann & Ferland 1993). Among relatively nearby ($z \lesssim 0.05$) AGN, Narrow-Line Seyfert 1s show evidence of large N abundances (e.g., Wills et al. 1999). It is, therefore, interesting that the X-ray spectra of NGC 3516, a low-redshift, Broad-Line Seyfert 1 galaxy, also shows evidence for an overabundance by a factor of 2 –3 of nitrogen in the central regions of the galaxy, with respect to other heavy elements. Furthermore, Kinkhabwala et al. (2002) presented evidence for a similar enhancement of nitrogen in the prototypical Seyfert 2 galaxy NGC 1068. Also, based on the strength of the N V λ1240 line, there is evidence of anomalous N abundances in the NLRs of the Seyfert 1 galaxies NGC 5548 (Kraemer et al. 1998) and NGC 4151 (Kraemer et al. 2000), although this could be at least partly due to enhanced emission by photo-excitation.

Nitrogen can be synthesized from carbon and oxygen produced within a star, referred to as primary production, or via the CNO process in intermediate mass stars (M $\lesssim$ 7 M$_\odot$; see Maeder & Meynet 1989) which already possess C and O, i.e., secondary production (e.g., Tinsley 1980). At certain temperatures N is enhanced at the expense of C (while at higher temperatures it would be at the expense of O). Thus it is possible to observe solar O, Ne etc yet obtain enhanced N with subsolar C. The enrichment of nitrogen via secondary production increases with overall metallicity such that N/H $\propto$ (O/H)^2 $\propto$ Z^2. Since the evidence for overabundant nitrogen is typically the high ratios of N lines to those of C or other heavy elements, one might expect that a factor of 3 enhancement of N/O would require Z $\sim$ 3 and N/H $\sim$ 9 times solar! However, for Z $\sim$ 1, it is still possible to have N/H a few times solar, assuming the enhancement of nitrogen is accompanied by a loss of carbon and, possibly oxygen (e.g. Maeder & Meynet 1989). For example, assuming roughly solar initial

abundances (Grevesse & Anders 1989), N/H could be 2.5 times solar if approximately half of the carbon were used up in the production of nitrogen. Interestingly, our models with solar carbon abundance overpredicted the strength of the Cvi Lα line by a factor of ~ 1.5. To explore the possibility that some of the carbon was lost in the production of nitrogen, we generated a third model, with the carbon abundance set to 47% solar (to fully account for the enhancement of nitrogen) and all other model parameters kept identical to those of Model 2. The predicted line fluxes for Model 3, scaled to the Ovii f-line, are listed in Table 2. The Cvi Lα line is now within the measurement errors, while the predictions for the other lines are essentially unchanged from those of Model 2. Hence, the emission-line fluxes are consistent with emission from photo-ionized gas in which the nitrogen is enhanced and the carbon depleted by the same amount. If the anomalous N/O and N/H ratios are consistent with Z ~ 1 and are the result of nitrogen production in intermediate mass stars, these results provide tight constraints on the history of star formation in the nucleus of NGC 3516.

6. Conclusions

We have used *XMM-Newton* RGS grating spectral data to examine the physical conditions within the X-ray emission-line gas in the Seyfert 1 galaxy NGC 3516. The spectra show emission-lines from the He-like ions of N, O and Ne, and H-like ions of C, N, and O. Also, we have detected RRC from Cvi and Oviii. We have shown the following:

1. The RGS data show the soft X-ray absorber to be consistent with the UV absorbers detected in earlier *HST*/STIS observations. However, the UV absorbers cannot account for the X-ray line emission. Although the UV absorbers could account for some of the Nvi and Ovii emission, they are generally too low an ionization state to produce any of the higher ionization lines detected in the RGS spectra. Furthermore, if the emission from the UV absorbers were scaled to fit the Ovii f component, the models predict Ovi $\lambda\lambda$ 1032,1038 lines almost an order of magnitude stronger than observed in a recent *FUSE* spectrum. While some line variability may occur, an order of magnitude change in Ovi between the *FUSE* observation and the epoch reported here is highly unlikely.

2. From the Cvi RRC, we find $kT \lesssim 0.01$ keV, consistent with low temperature ($\lesssim 10^5$ K), photoionized gas. Based on the ratios of the f- and i- lines from He-like Ovii and the relative strength of Nvi f, we suggest that the gas is in the low-density regime ($n_e \lesssim 10^8$ cm^{-2}). We have been able to fit the observed emission-line ratios with a single zoned photoionization model, with N$_H$ = 1.5 x 10^{21} cm^{-2} and $U = 1.1$, however, in the case of solar abundances, the Nvi and Nvii lines are significantly underpredicted. Hence, we suggest that the N/H ratio is at least 2.5 times solar, which may be the result of secondary production

of nitrogen in intermediate mass stars. Follow-up observations of the stellar population in the nucleus of NGC 3516 could help test this possibility.

3. In order to produce the observed OVII line fluxes, the emission-line gas must have a global covering factor of ~ 0.5. The scaled (predicted) OVI $\lambda\lambda$ 1032, 1038 emission is slightly higher than that seen in the *FUSE* spectrum, although the OVI line ratios and profiles show strong evidence for absorption, possibly from an additional component of UV absorption near systemic that cannot be deconvolved from the strong UV components seen in the STIS spectra. Hence, the X-ray model is generally consistent with the *FUSE* spectrum.

7. Acknowledgements

Table 1.   RGS Emission Line Measurements

Energy[a]	ID	Line[b]	Flux1 [c]	Flux2 [d]
0.3671	CviLyα (0.366)	46 ± 15	1.85	1.08
0.4198	Nvi$f$ (0.4198)	119 ± 17	3.18	2.13
0.4280	Nvi $i+r$ (0.4263/0.4307)	41 ± 13	1.69	1.16
0.4913	Cvi RRC (0.4900)	29^{+10}_{-11}	3.35	2.63
0.5004	Nvii (0.5002)	37 ± 14	1.06	0.85
0.5614	Ovii(f) (0.5610) [e]	122 ± 17	4.21	3.78
0.5681	Ovii(i) (0.5686) [e]	30 ± 12	1.20	1.09
0.5727	Ovii(r) (0.5739) [e]	49 ± 12	1.38	1.27
0.6540	Oviii (0.6510)	48 ± 12	0.82	1.31
0.9047	Neix f (0.9055) [f]	25^{+10}_{-9}	0.57	0.83

[a]The measured rest-energy of the line in keV, corrected for the systematic velocity of the host galaxy

[b]Counts attributed to the line (after subtraction of the continuum flux). Errors are 1 σ

[c]Total photons cm^{-2} s^{-1} in the line in units 10^{-5}. Lines assumed to have widths FWHM= 650 km/s

[d]Line flux as ergs cm^{-2} s^{-1} in the line in units 10^{-14}

[e]RGS 1 only

[f]RGS 2 only

Table 2. Predicted Emission-Line Fluxes[a]

Line	Model 1[b]	Model 2[c]	Model 3[d]	Measured
CvɪLyα	1.55	1.57	0.87	1.08 ± 0.35
Nvɪf	0.57	1.43	1.44	2.13 ± 0.30
Nvɪ $i+r$	0.48	0.86	0.86	1.16 ± 0.37
Nvɪɪ	0.53	1.10	1.19	0.85 ± 0.32
Ovɪɪ(f)	3.78	3.78	3.78	3.78 ± 0.53
Ovɪɪ(i)	0.94	0.94	0.94	1.09 ± 0.44
Ovɪɪ(r)	1.03	1.03	1.04	1.27 ± 0.31
Ovɪɪɪ	1.30	1.27	1.30	1.31 ± 0.33
Neɪx f	0.89	0.90	0.89	0.83 ± 0.33

[a]Fluxes as ergs cm^{-2} s^{-1} in units of 10^{-14}.

[b]Solar abundances. Fluxes scaled to the O VII f-line.

[c]N/H $\sim$ 2.5 times solar. Fluxes scaled to the O VII f-line.

[d]N/H $\sim$ 2.5 times solar; C depleted to 47% relative to solar. Fluxes scaled to the O VII f-line.
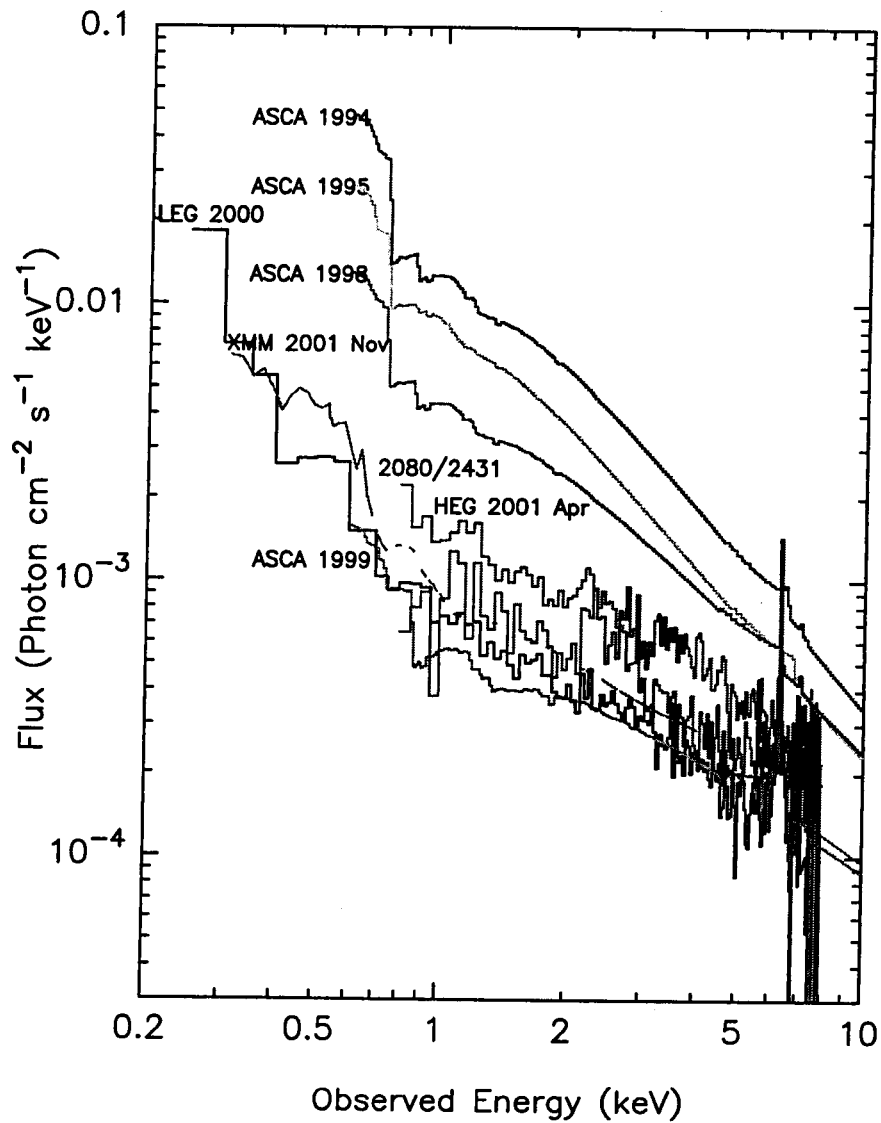
Fig. 1.— An X-ray flux history for NGC 3516. Schematic models are shown representing the X-ray flux levels observed by recent satellites. The data show NGC 3516 to be close to the lowest flux state on record, also observed by the LETG and by *ASCA* in 1999. HEG spectra from two observation intervals 2001 April are represented, as are lines showing the source at a much higher flux state, as observed by *ASCA*
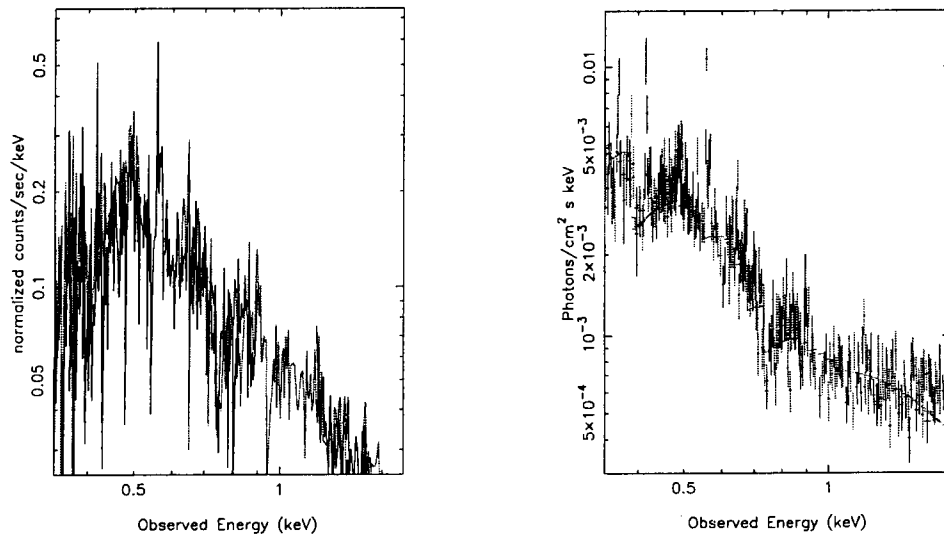
Fig. 2.— Left: The RGS data with errors removed for clarity of viewing. The red line represents R2, the black line represents R1. The data points are connected by a line, the gaps evident in one section of each RGS are due to loss of functionality in some CCD chips. Right: The unfolded RGS 1 and 2 data (red) compared to a powerlaw model attenuated by the absorbing column indicated by UV data (green line)
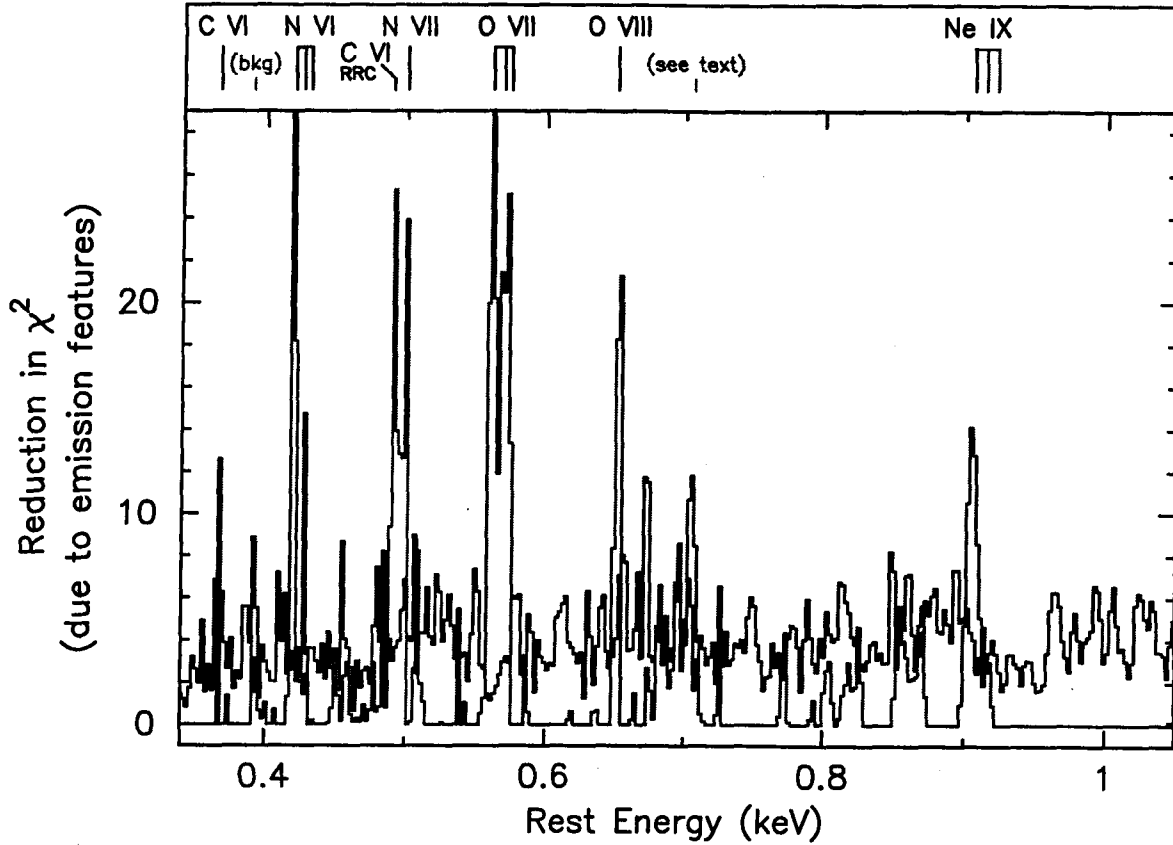
Fig. 3.— Illustration of the significance of emission features. The red histogram shows the reduction in χ^2 of the fit to the observed data when a narrow emission line is added to our model of the continuum at each energy. The data for the Nvi and Ovii lines are truncated; the peaks are actually at 31 and 87, respectively. No significant emission features were found above 1 keV. The blue histogram shows the maximum reduction in χ^2 obtained at each energy when an identical analysis is performed on 20 sets of simulated spectra (see text). This histogram therefore represents the 95% confidence threshold for narrow emission features. The lines listed in Table 1 are marked, along with other features discussed in the text. It should be stressed that this plot conveys the change in statistic, *not* the intensity of the putative line.

REFERENCES

Blustin, A., et al. 2002, A&A, 392, 453

Branduardi-Raymont, G., Sako, M., Kahn, S.M., Brinkman, A.C., Kaastra, J.S., Page, M.J., 2001, A&A 365, L140

Crenshaw, D.M., et al. 2001, ApJ, 555, 633

Crenshaw, D.M., Kraemer, S.B., Gabel, J.R., Kaastra, J.S., Steenbrugge, K., George, I.M., Turner, T.J., Yaqoob, T., & Dunn, J.P. 2003, submitted to ApJ

den Herder, J. A. et al. 2001, A&A, 365, 7

Grevesse, N., & Anders, E. 1989, in Cosmic Abundances of Matter, ed. C.J. Waddington (New York: AIP), 1

Ferland, G.A., Korista, K., T., Verner, D.A., Ferguson, J. W., Kingdon, J. B., Verner, E. M. 1998, PASP, 110, 761

Ferruit, P., Wilson, A.S., Mulchaey, J.S. 1998, ApJ, 509, 646

Hamann, F., & Ferland, G. 1993, ApJ, 418, 11

Hutchings,J.B., et al. 2001, ApJ, 556, L21

Keel, W.C., 1996, AJ, 111, 696

Kinkhabwala, A., et al. 2002, ApJ, 575, 732

Kraemer, S.B., & Crenshaw, D.M. 2000, ApJ, 544, 763

Kraemer, S.B., Crenshaw, D.M., Filippenko, A.V., & Peterson, B.M. 1998, ApJ, 499, 719

Kraemer, S. B., Crenshaw, D. M., George, I. M., Netzer, H., Turner, T. J., Gabel, J. R., 2002, ApJ, 577, 113.

Kraemer, S.B., Crenshaw, D.M., Hutchings, J.B., Gull, T.R., Kaiser, M.E., Nelson, C.A., & Weistrop D. 200, ApJ, 531, 278

Kriss, G. A. et al. 1996, ApJ, 467, 629

Liedahl, D.A. 1999 in X-ray Spectroscopy in Astrophysics, EADN School proceeding, 1997, ed. J.A. van Paradijs & J.A.M Bleeker, 189

Maeder, A., & Meynet, G. 1989, A&A, 210, 155

Mewe, R. 1999 in X-ray Spectroscopy in Astrophysics, EADN School proceeding, 1997, ed. J.A. van Paradijs & J.A.M Bleeker, 109

Netzer, H., Chelouche, D., George, I. M., Turner, T. J., Crenshaw, D. M., Kraemer, S. B., Nandra, K., 2002, ApJ, 571, 256

Pradhan, A.K. 1985, ApJ, 288, 824

Porquet, D., & Dubau, J. 2000, A&AS, 143, 495

Sako, M., Kahn, S.M., Paerels, F., Liedahl, D.A., 2000, ApJ, 543, 115

Sako, M., et al. 2001, A&A, 365, 168

Shields, G.A., & Kennicutt, R.C. 1995, ApJ, 454, 807

Snow, T.P., & Witt, A.N. 1996, ApJ, 468, L65

Tinsley, B.M. 1980, Fund. Cos. Phys., 5, 287

Turner, T.J., Mushotzky, R.F., Yaqoob, T., George, I.M., Snowden, S.L., Netzer, H., Kraemer, S.B., Nandra, K., Chelouche, D., 2002, ApJ, 574, 123

Wills, B., Brotherton, M.S., Laor, A., Wills, D., Wilkes, B.J., Ferland, G., & Shang, Z. 1999, in ASP Conf. Ser. 162, Quasars and Cosmology, ed. G. Ferland & J. Baldwin (San Francisco: ASP), 161